Hindawi

Research Article

Effect of Friction Coefficient in Friction Stir Welding of B4C Reinforced AA5083 Metal Matrix Composites and Use of Fuzzy Clustering Technique for Weld Strength Prediction

C. Devanathan [ID],[1] **D. Elil Raja** [ID],[2] **Tushar Sonar** [ID],[3] **and Mikhail Ivanov** [ID][3]

[1]*Department of Mechanical Engineering, Rajalakshmi Engineering College, Chennai 602105, Tamil Nadu, India*
[2]*Department of Mechanical Engineering, St. Joseph's Institute of Technology, OMR, Chennai, Tamil Nadu 600119, India*
[3]*Department of Welding Engineering, Institution of Engineering and Technology,*
 South Ural State University (National Research University), Chelyabinsk 454080, Russia

Correspondence should be addressed to D. Elil Raja; elilraja76@gmail.com

The friction stir welding (FSW) method was used to weld B4C reinforced AA 5083 metal matrix composites in this study. By coating titanium nitride (TiN), aluminium chromium nitride (AlCrN), and diamond-like carbon (DLC) to a thickness of 4 microns, three FSW tools with square pin profiles were developed and the friction coefficients of 0.69, 0.32, and 0.2 were maintained. At three levels, the process factors such as tool rotating speed, transverse feed, and axial force were examined. For each tool, 15 samples were made using the central composite design. The influence of the friction coefficient on ultimate tensile strength, microstructural features, and tool condition was studied, and the flower pollination algorithm (FPA) technique was used to find the best process parameters for obtaining maximum ultimate tensile strength of FSW joints. The improved tensile strength of FSW joints was verified using a validation test. The coating has a considerable influence on the ultimate tensile strength, microstructure, and tool condition, according to the results of the tool's friction coefficient. The results on the prediction of strength using the fuzzy clustering technique showed that the technique is effective in predicting the tensile strength values, with the root mean square error (RSME) of TiN, AlCrN, and DLC being 0.0027, 0.0016, and 0.0015, respectively, and the low RSME indicating that the prediction based on the fuzzy subtractive clustering technique is perfect and effective.

1. Introduction

In order to meet good fuel economy, automobile manufacturers are increasingly moving towards metal matrix composites (MMCs). Most of the models in modern automobiles including Lotus Elise, General Motors EVI, Chrysler Prowler, Volkswagen, and Toyota have used metal matrix composites for manufacturing their automobile parts [1]. The composite's desired qualities are achieved by combining the reinforcement's strength with the ductility of the matrix material. Despite the fact that MMCs have existed since the 1960s, the materials have yet to be fully commercialized due to their higher manufacturing costs and a lack of knowledge of the material's performance at extreme temperatures [2]. Fusion joining, solid-state joining, and other similar methods are used

to join the composite materials. There are a few challenges that must be overcome during the fusion welding of composite materials, particularly particulate-reinforced MMCs, such as melting above the melting point, the high viscosity of the melt, matrix, and reinforcement interaction, gas evolution, and segregation during solidification. The friction stir welding (FSW) process has shown potential benefits in minimzing the fusion welding related problems of aluminium alloys. Gopalakrishnan et al. [3] used a mathematical model that includes welding factors such as axial force, tool revolving speed, traverse feed, additional reinforcement %, and tool pin shape to predict the tensile strength of the specimen connected. In his research, TiC particles are used to reinforce the AA 6061 material. The efficiency of the joint achieved in the majority of the joints created was greater than 90%. The profile of the tool

pin was shown to be more dominant than other characteristics in the established model. Several studies have recently attempted FSW process for joining various metal and composite materials [4–6]. Parikh et al. [7] attempted to examine the articles on the FSW of metal matrix composites that were accessible. His thorough examination found that research including multiobjective optimization of process parameters in FSW will improve the utilization of composites in manufacturing. Tool wear, particularly the pin section of the tool, is still a major issue that must be addressed.

Hassen et al. investigated the wear behaviour of the welded connection while welding hybrid composites using various process parameters and pin profiles. The square pin tool had better wear resistance, which increased as the traverse feed was increased and the rotating speed was reduced in the experiments [8]. Various base materials, such as AA6061, AA7005, and AA2124, were strengthened with Al_2O_3, SiC, TiB_2, B_4C, and ZrB_2, and joined by friction stir welding [9–14].

Ali et al. [15] focused on studying the process parameter effect on properties of friction stir welded AL 6061 metal matrix composites reinforced with different SiC and B_4C particles. The test results showed that the maximum tensile strength of value 174 MPa was obtained for 10% SiC and 3% B_4C composites. The percentage elongation increases with increasing B_4C and decreases with reducing the SiC components. The wear resistance increases with the addition of reinforcement in Aal-metal matrix composites and the wear rate increases with an increase in load.

Prasad et al. [16] made an attempt to join 5 mm thick AA6061 T6 and AA6351-T6 aluminium dissimilar plates. The welded surfaces were free from cracks and the maximum tensile strength of 167.95 MPa was reported for the square tool pin. Yadav et al. [17] performed an experimental and numerical study in the thermal field and characteristics of the weld during submerged arc welding. The model controls the melting and solidification phases during welding. The microstructural investigation was also carried out in which the various distinct zones were clearly visible. Hasan et al. [18] fabricated copper alloy Bronze RG 10 reinforced with TiC and graphite to improve the wear behaviour by powder metallurgy route. The results showed significant decrease in the wear rate when increasing the percentage of TiC and graphite. The composites were best suited for coupling parts in the aerospace and automobile sectors.

Rao et al. [19] focused on the aging assessment of transformer insulation oil based on the integrated design of a fuzzy clustering system and found that the methodology adopted was effective and efficient in classifying the age group of the oil. Ali et al. [20] proposed the use of a subtractive fuzzy clustering technique for modeling soil cation exchange capacity and the results showed that the fuzzy subtractive clustering algorithm had high accuracy in predicting and modeling soil ratio exchange capacity. Yazdani Chamzini et al. [21] used the fuzzy model-based subtractive clustering technique to predict the performance of road header. The Takagi–Sugeno (TS) fuzzy system based on the subtractive clustering method was effective and capable in finding the complex relationship between road header and other parameters.

Pathak and Adhyaru [22] used model reference adaptive control based fuzzy subtractive clustering method to control the motion parameters of DC servo motor. The results showed that FSC is more efficient and effective in reading the chattering and error convergence. It was observed from the literature that the fuzzy clustering technique was less applied in predicting mechanical properties. In the present work, an attempt was made to apply the fuzzy subtractive clustering technique to predict the tensile strength of the welded specimen.

The B_4C-reinforced aluminium MMCsare widely used in bullet-proof vests, bicycle frames, armor tanks, nuclear waste containment, neutron absorbers in nuclear power plants, and many transportation applications. The use of the material in these applications requires the joining with the same or different materials using different joining methods. From the literature study, it was noticed that only limited work has been reported in the joining of B4C-reinforcedAA 5083 MMCs. The novelty of this research article resides in analyzing the weld characteristics in terms of effect of friction coefficient and use of the flower pollination algorithm (FPA) technique to find the best process parameters for maximizing and predictingthe ultimate tensile strength of friction stir welded B4C reinforced AA5083 MMC joints using the fuzzy clustering technique.

The main objective of this research article is to study the influence of the friction coefficient on ultimate tensile strength and microstructural features of FSW joints and analyzing the FSW tool condition after welding. The flower pollination algorithm (FPA) technique was used to find the best process parameters for obtaining maximum ultimate tensile strength of FSW joints.

In this proposed research work, the AA5083 alloy reinforced with 10% volume fraction of boron carbide MMCs were made using liquid stir casting process with dimensions of $10\,cm \times 5\,cm \times 0.6\,cm$. Using a CNC milling machine, the composites are machined to the desired specifications. The produced composites were joined using a solid state friction stir welding (FSW) procedure with three distinct ranges of tool rotational speed, traverse feed, and axial force. Three tools with square pin profile were fabricated andcoated with TiN, AlCrN, and DLC to a thickness of four microns for changing the friction coefficient and wear resistance of FSW tool.

Figure 1 depicts the suggested work plan as a flow chart. In the experimental Sections 2.1 and 2.2, the specifics of the process parameter selection, tool design and coating, composite preparation, and experimentation are described. Part 1 discussion is offered as 3.1, 3.2, and 3.3 in the findings and discussion section. The observed UTS values were used to train fuzzy clustering to predict the strength which was explained in Section 3.4.

2. Experimental Procedure

2.1. Selection of Materials. The basis material was nonheat treatable medium strength aluminium AA 5083, which has uses in crucial arctic, maritime structures, storage, and transportation tanks for cryogenic fluids. The stir casting
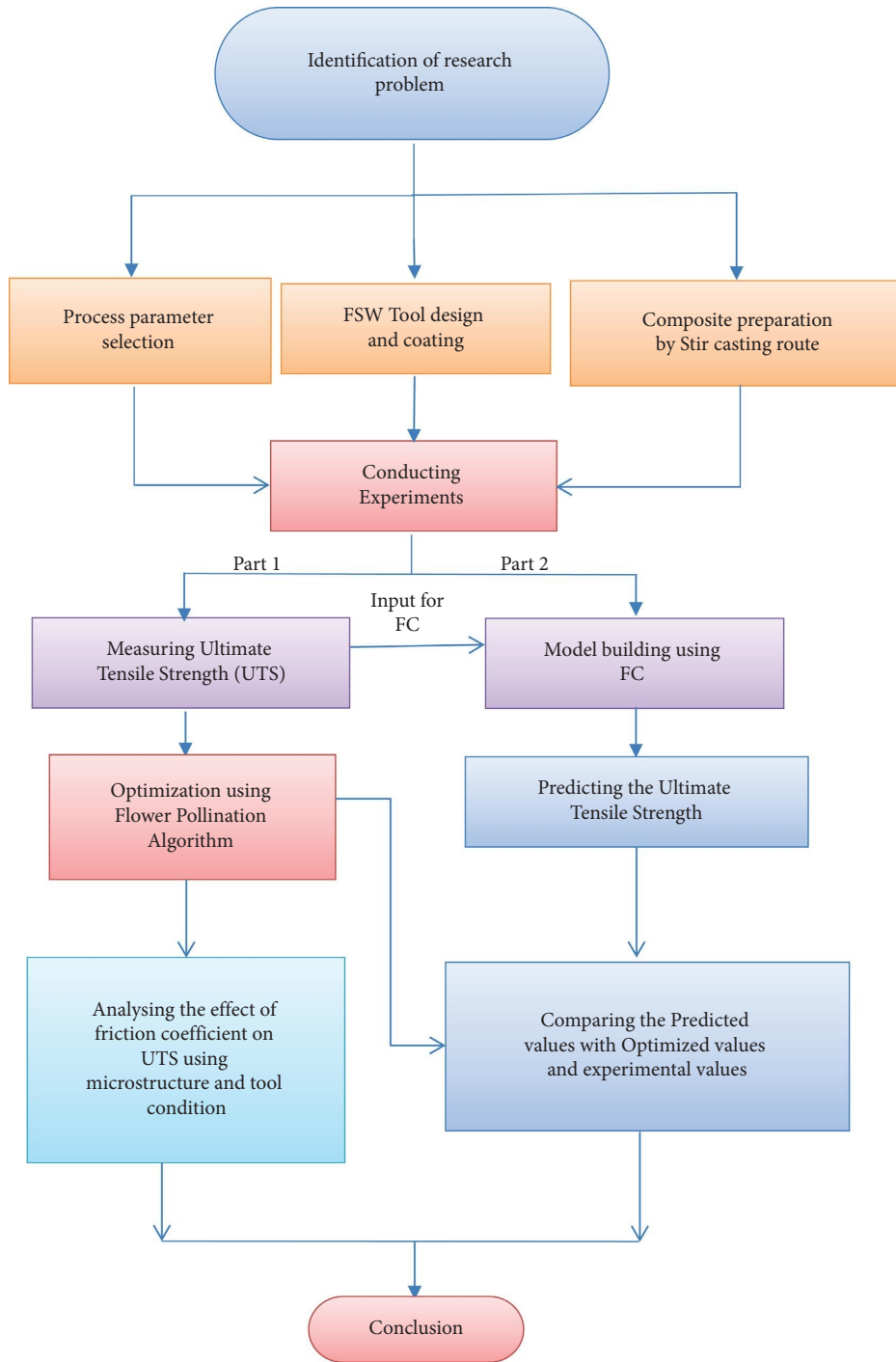
FIGURE 1: Plan of the proposed work as a flow chart.

process was used to manufacture composite blocks reinforced with a boron carbide particle with an average particle size of 10 microns in AA 5083 to a 10% volume fraction. Liquid stir casting is one of the most appropriate technologies for producing composites with a volume fraction of up to 30%. A crucible was used to melt the AA 5083 aluminium alloy in an electrical furnace. To make metal matrix composites, weighed amounts of B_4C particles were added to molten aluminium metal. To guarantee equal particle dispersion in the molten metal, a mechanical stirrer with an electric motor was used to agitate the melt. The temperature of the molten metal was kept at 850°C during the composites' preparation, and it was placed into a prepared die and allowed to harden. The die was made of hot wrought steel and was 10.5 cm × 10.5 cm × 0.8 cm in size. The composite blocks were visually examined for surface flaws before being cut to a size of 10.4 cm × 5 cm × 0.6 cm using a vertical milling machine. Figure 2 depicts the sample composite blocks.

FIGURE 2: Sample composite blocks.

The tool is a critical component in creating a defect-free weld in friction stir welding. The spinning tool's primary duty is to heat the base material and to allow it to flow in both horizontal and vertical directions. It was clear from the literature that pins with a square shape provided defect-free welding. The tool material's friction coefficient has an effect on heat generation and material flow characteristics.

Three tools were machined and coated with TiN, AlCrN, and DLC to change their hardness and friction coefficient. The basic characteristic of the coating is given in Table 1.

2.2. Conducting the Experiments. Rotational speed, traverse feed, and axial force were used as process variables in this study and were measured in three distinct ranges. Table 2 lists the process parameters and their ranges.

The number of experiments was determined using the formula $2^k + 2K + C$, where C is the number of central points and K is the number of factors considered [23]. Using a computer-controlled FSW machine, a total of 15 trials were carried out for each coated tool.

3. Results and Discussion

3.1. Ultimate Tensile Strength (UTS). Tensile strength is one of the most important properties for determining a material's mechanical performance, particularly for freshly created materials such as composites. The welded workpieces were visually inspected for surface problems before samples were machined using the wire EDM method to test the ultimate tensile strength

according to ASTM E8 standards with 32 mm gauge widths of 6 mm gauge lengths and overall lengths of 100 mm. The specimens were put through their paces in a computerized UTM with a load capacity of 100 kN. Figure 3 depicts the samples of welded joint's tensile test specimen joined using the AlCrN-coated tool after the test.

From the tested specimens, it was noticed that specimens joined using the AlCrN-coated tool failed at the heat affected zone, whereas the specimens joined using the DLC-coated tool failed at the stir zone which indicates that stirring was not proper and due to which tensile strength was affected. It was observed from the test results that the specimens which got a break at the heat affected zone had resulted in better tensile strength and the components that failed at the stir zone had resulted in lower tensileAlCrN coated.

The AlCrN-coated tool had the highest ultimate tensile strength of 153 MPa, followed by the TiN-coated tool with 136 MPa and the DLC-coated tool with 130 MPa, according to the experimental data. Figure 4 depicts the ultimate tensile strength findings. The experimental results demonstrated that the fluctuation of UTS was minimal for all the three coated tools, with a significant difference between them. This implies that the discrepancy is attributable to a difference in the tool coating friction coefficient.

Design expert 12.0 version software was used to create the mathematical model for all the three coated tools. For TiN-, AlCrN-, and DLC-coated tools, the model equation in the coded form is given in equations (1)–(3), respectively.

TABLE 1: Characteristics of the coating.

Coating type	Coated tool	Characteristics of coating
TiN		Colour: gold Average hardness: 2300 Hv Friction coefficient: 0.69 Coating thickness: 4 microns
AlCrN		Colour: gray Average hardness: 3100 Hv Friction coefficient: 0.35 Coating thickness: 4 microns
DLC		Colour: black Average hardness: 3500 Hv Friction coefficient: 0.2 Coating thickness: 4 microns

TABLE 2: Process parameters and their range.

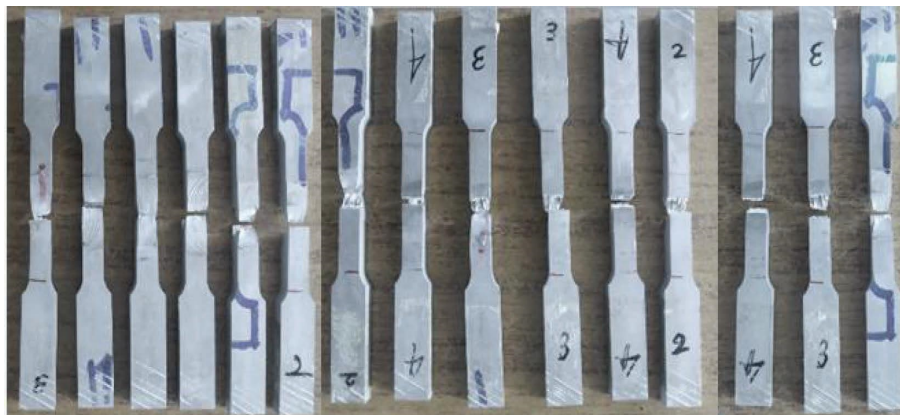| Serial no.	Welding parameter	Symbol	Unit	Level 1	Level 2	Level 3
1	Rotational speed	A	Rpm	1200	1500	1800
2	Traverse feed	B	mm/min	20	40	60
3	Axial force	C	kN	6	7	8

FIGURE 3: Sample tensile test specimen after the test.

$$\text{UTS} = 134.50 - 0.0175\,A + 1.14\,B - 0.5637\,C + 0.2900\,AB + 1.23\,AC + 2.04\,BC - 2.90\,AA - 2.04\,BB - 0.3721\,CC, \quad (1)$$

$$\text{UTS} = 151.03 + 0.4287\,A + 0.0800\,B - 0.4513\,C - 1.000\,AB - 1.09\,AC - 1.05\,BC - 1.22\,AA + .1563\,BB - 0.1363\,CC, \quad (2)$$

$$\text{UTS} = 128.97 + 0.2325\,A - 0.3063\,B + 1.27\,C - 0.225\,AB - 1.24\,AC + 1.14\,BC - 2.18\,AA - 1.09\,BB - 1.49\,CC. \quad (3)$$

In this investigation, the F ratio for the titanium nitrate-coated tool is 19.60, with a 0.0496 discrepancy between anticipated and adjusted R^2. The P value of the TiN-coated tool is 0.0022. The diamond-like carbon-coated tool has an F ratio of 35.58, a difference of 0.0276, and a P value of 0.0005, whereas the aluminium chromium nitrate-coated
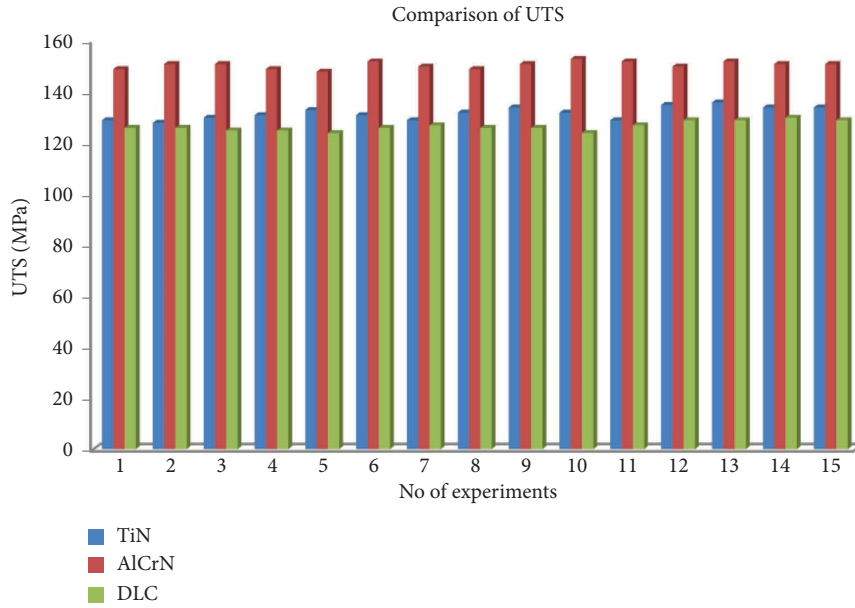
Figure 4: Comparison of UTS among three tools.

tool has an F ratio of 11.39, a difference of 0.064, and a P value of 0.0077. The ANOVA test results for the tensile strength of all three tools are shown in Table 3.

3.2. Optimization Using the Flower Pollination Algorithm.

The flower pollination algorithm is a nature-inspired metaheuristic algorithm that replicates pollination behaviour in blossoming plants. Yang developed this approach in 2012, and it outperforms other metaheuristic algorithms [24]. The flower pollination approach was utilized in this research to get the best ultimate tensile strength values. The MATLAB R 2018a version program was used to estimate the ideal ultimate tensile strength and its associated process parameters. A confirmation test was performed on the improved settings, with the results compared to the expected values.

3.3. Microstructural Investigation.

The microstructural analysis was carried out in this study for the joints that provided the highest and least tensile strength with all three coated tools. The maximum strength was 136 MPa for the process parameters of rotational speed 1500 rpm, traverse feed 40 mm/min, and axial force 7 kN, according to the findings of the tensile test.

The welded component joined by the TiN-coated tool was examined under a microscope with a magnification range of 5x–300,000x and an accelerating voltage of 0.3–30 Kv, using a Hitachi SU1510 model with a magnification range of 5x–300,000x.

The welded specimen's base material is shown in Figure 5(a). The boron carbide particles were uniformly dispersed, as seen in the diagram. A small aggregation of particles was observed in a few sites. The different zones of friction stir welding have been seen in Figures 5(b)–5(d).

The grains were elongated and deformed patches were detected in the agitation zone of the specimen due to plastic deformation, as illustrated in Figure 6(c). The process

Table 3: ANOVA test results of UTS.

Particulars		Tool coating		
		TiN	AlCrN	DLC
Sum of squares	Regression	79.32	21.96	52.35
	Residual	2.25	1.07	0.8173
Mean squares	Regression	8.81	2.44	5.82
	Residual	0.4496	0.2141	0.1635
Degrees of freedom	Regression	9	9	9
	Residual	5	5	5
F ratio		19.60	11.39	35.58
P value		0.0022	0.0077	0.0005
R^2 value		97.24	93.35	98.46
Adjusted R^2 value		92.28	86.95	95.70
Remarks		Significant	Significant	Significant

settings of 1800 rpm, 20 mm/min, and 7 KN resulted in unsatisfactory strength, as illustrated in Figures 5(e) and 5(f).

This happened because the TiN-coated tool had a lower hardness and a greater friction coefficient. The amount of heat generated during the process for this combination was high due to the higher friction coefficient, higher rotational speed, and lower traverse feed, causing the aluminium particles to become stuck on the tool materials' surface, resulting in small voids and tunnels in the weld zone, as shown in Figures 5(e) and 5(f).

Figures 6(a)–6(d) show the optical images taken corresponding to the specimen which produced the maximum strength of 153 MPa for 1500 rpm, 40 mm/min, and 7 kN using the AlCrN-coated tool. During the process, stirring was effective due to the nominal value of friction coefficient and hardness. The distinct regions such as stir zone, TMAZ, and HAZ are clearly shown. The onion rings were formed near the stir zone due to the frictional heat generated by the

Mag: 200x

(a)

Mag: 200x

(b)

Mag: 200x

(c)
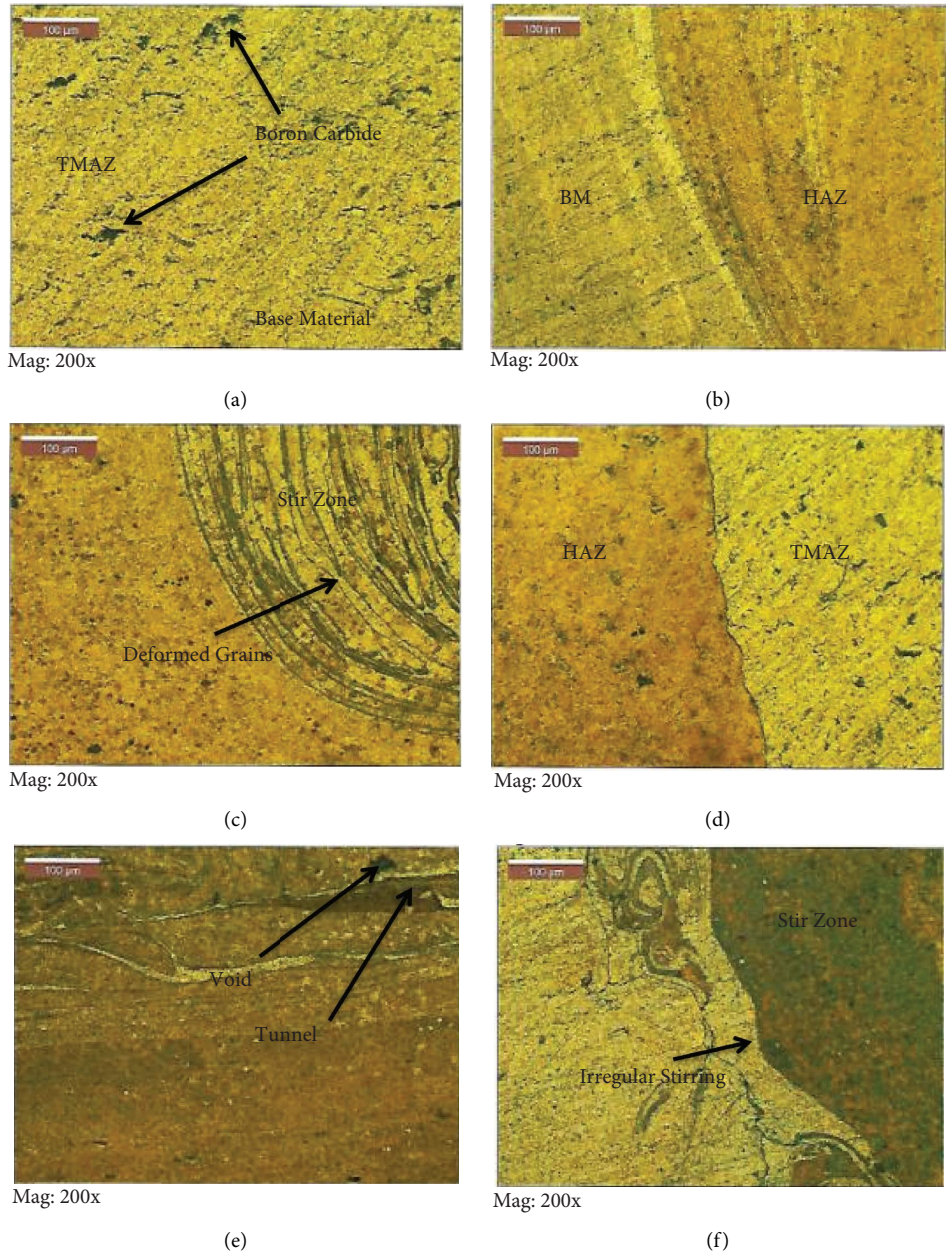

Mag: 200x

(d)

Mag: 200x

(e)

Mag: 200x

(f)

FIGURE 5: (a) Base material with B4C particles, (b-d) Different microstructural regions of specimen prepared by the TiN-coated tool at 1500 rpm, 40 mm/min, and 7 kN (e) and (f) at 1800 rpm, 20 mm/min, and 7 kN.
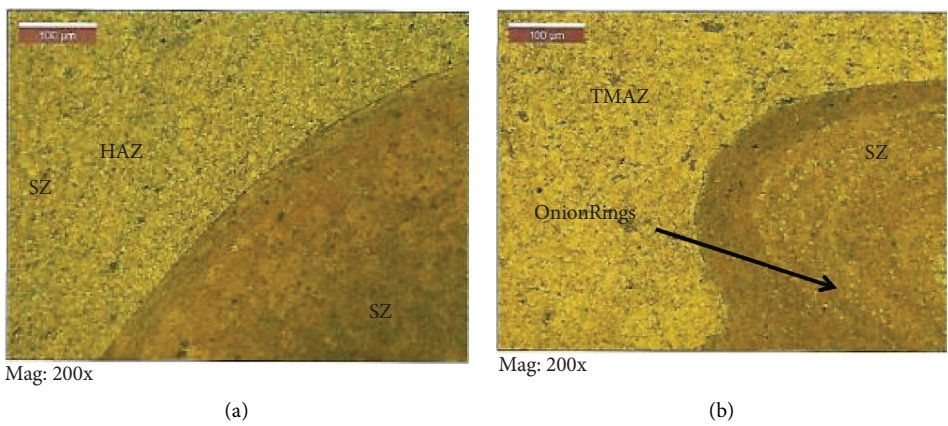

Mag: 200x

(a)

Mag: 200x

(b)

FIGURE 6: Continued.
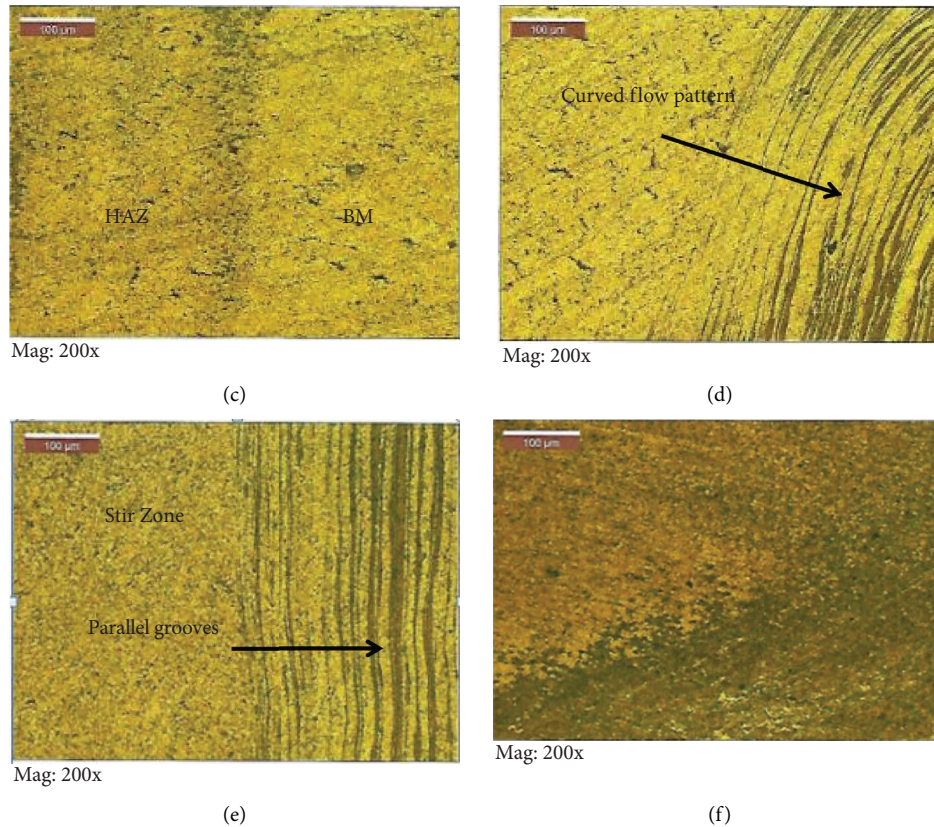
(c)

(d)

(e)

(f)

FIGURE 6: (a-d) Different microstructural regions of a specimen prepared by the AlCrN-coated tool at 1500 rpm, 40 mm/min, 7 kN (e) and (f) at 1200 rpm, 40 mm/min, and 6 kN.

rotating tool and the forward extruded movement of the metal. In this zone, the deformation in the longitudinal and transverse directions was different. Several researchers reported and discussed the formation of onion rings [25–30]. The images of poor strength had a parallel groove and an absence of clear distinct regions.

The optical microscopic images of the DLC-coated tool are shown in Figures 7(a)–7(f). Figures 7(a)–7(d) depict the images taken from the specimen with poor strength of 124 MPa at 1200 rpm, 40 mm/min, and 6 kN. Due to the low friction coefficient, the tool develops low heat during stirring which in turn affects the effective stirring of the process. Figures 7(a)–7(c) show that the stirring of the material is not proper and shiny and skinny surfaces were observed due to the slipping of the tool during stirring. Figures 7(e)–7(f) show the optical microscopic images of the specimen prepared for 1500 rpm, 40 mm/min, and 7 kN. The tensile strength measured for aforesaid parameters was 129 MPa. In the optical images, the various weld regions such as stir zone, heat affeted zone, and thermomechanically affected zone were observed clearly.

3.4. Condition of the Tool.
The FSW tool was subjected to one of the following three circumstances during the stirring process: maximum sliding, maximum sticking, and partial sliding and/or partial sticking. Images collected with the use of video-measuring equipment reveal that the aluminium particles became adhered to the surface of the TiN coated tool in the current experiment, as shown in Figures 8(a)–8(c). During the process, when the yield strength of the workpiece is less than shear stress produced in the contact area. Small segments of workpiece materials would stick to the tool surface which is considered as phenomenon called more sticking. The friction coefficient of the tool material greatly controls the amount of shear stress developed. Normally, a higher friction coefficient leads to the higher shear stress. In Figures 8(d)–8(f), it was noticed that white-colored materials were stick on side surface of the tool.

The pin of the DLC-coated tool, on the other hand, had completely worn out throughout the operation. The DLC-coated tool has a friction coefficient of roughly 0.2, resulting in a shear stress that is lower than the material's yield strength. The extrusion of the materials was carried out only by the pin in this condition of stirring, which is referred to as complete sliding. The pinned piece has completely worn away as a result of these circumstances.

Figure 9 shows an optical microscopic picture acquired to better understand the surface behaviour of the worn tool. The photograph was taken on the shoulder's upper surface, which is in touch with the workpiece materials. It has parallel grooves, indicating that it was worn during the manufacturing process.

3.5. Prediction Based on Fuzzy Clustering.
Soft computing approaches may be used to find solutions to complicated systems that are nonlinear, continuous, discrete, or dynamic

Mag: 200x

(a)

Mag: 200x

(b)

Mag: 200x

(c)

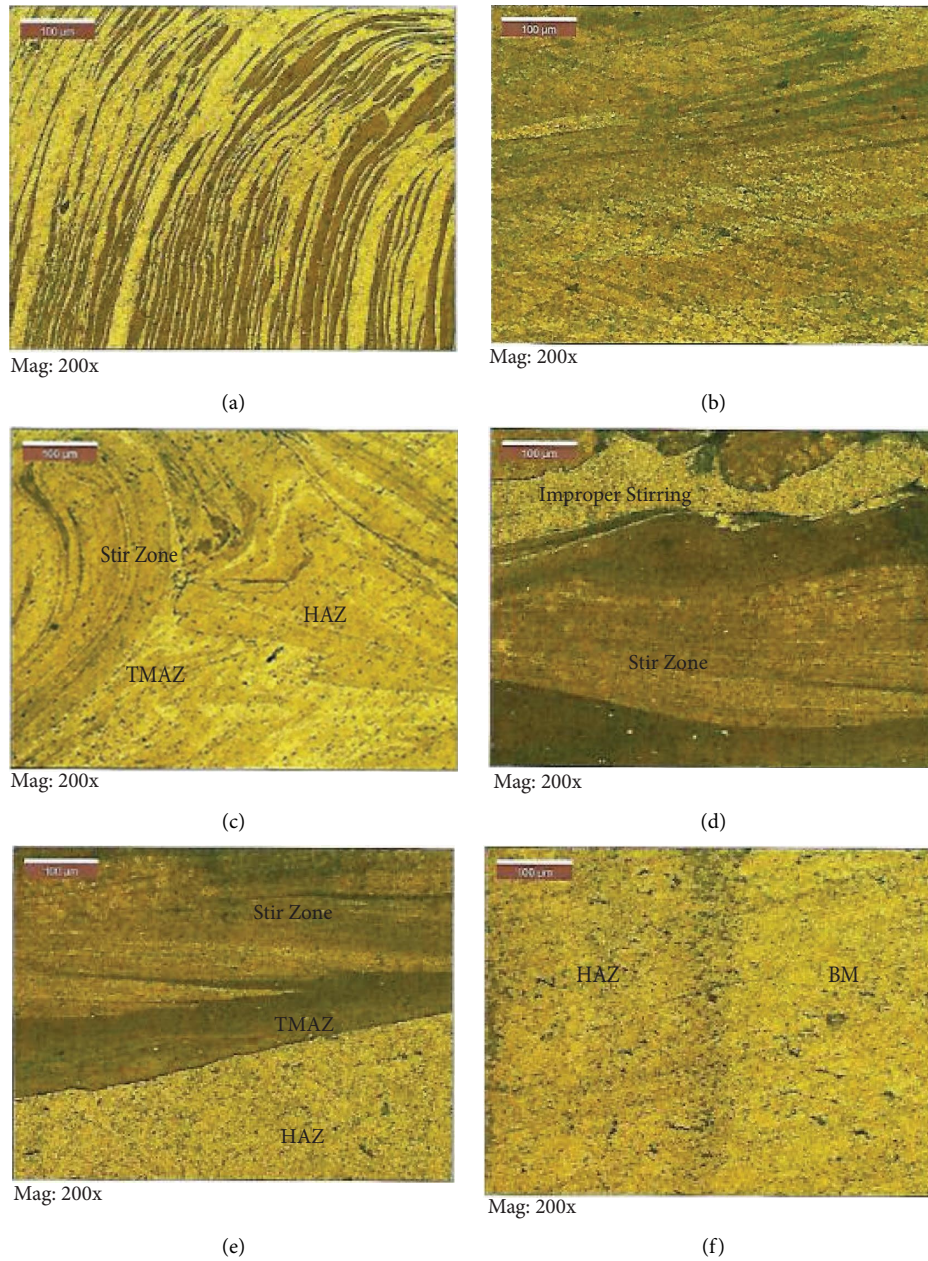Mag: 200x

(d)

Mag: 200x

(e)

Mag: 200x

(f)

FIGURE 7: (a-d) Different microstructural regions of specimen prepared by the DLC-coated tool at 1200 rpm, 40 mm/min, and 6 kN (e) and (f) at 1500 rpm, 40 mm/min, and 7 kN.

in nature. Soft computing, unlike hard computing, may provide effective solutions to complicated models utilizing approximation models. Prediction, categorization, and optimization approaches are all examples of soft computing techniques. Machine learning, fuzzy logic, artificial neural networks, genetic algorithms, and expert systems are examples of well-known and popular soft computing approaches [31]. Experiments to acquire huge sets of input and output data are time consuming, hence the fuzzy subtractive clustering approach is used in the provided study effort to forecast the ultimate tensile strength of three separate specimens.

System modeling may be done with fuzzy sets, which are sets having inaccurate or hazy bounds. The two major classes involved in the application fuzzy set known as fuzzy logic controller are linguistic fuzzy modeling and precise fuzzy modeling (FLC). Clustering, a strong data mining approach, is a powerful tool for extracting usable information from a set of data. After examining the dataset, the clustering algorithm divides the data into numerous clusters based on pattern similarities [32].

There are three primary processes in the fuzzy inference system based on Chiu's fuzzy subtractive clustering approach. In an M-dimensional space, for example, with data
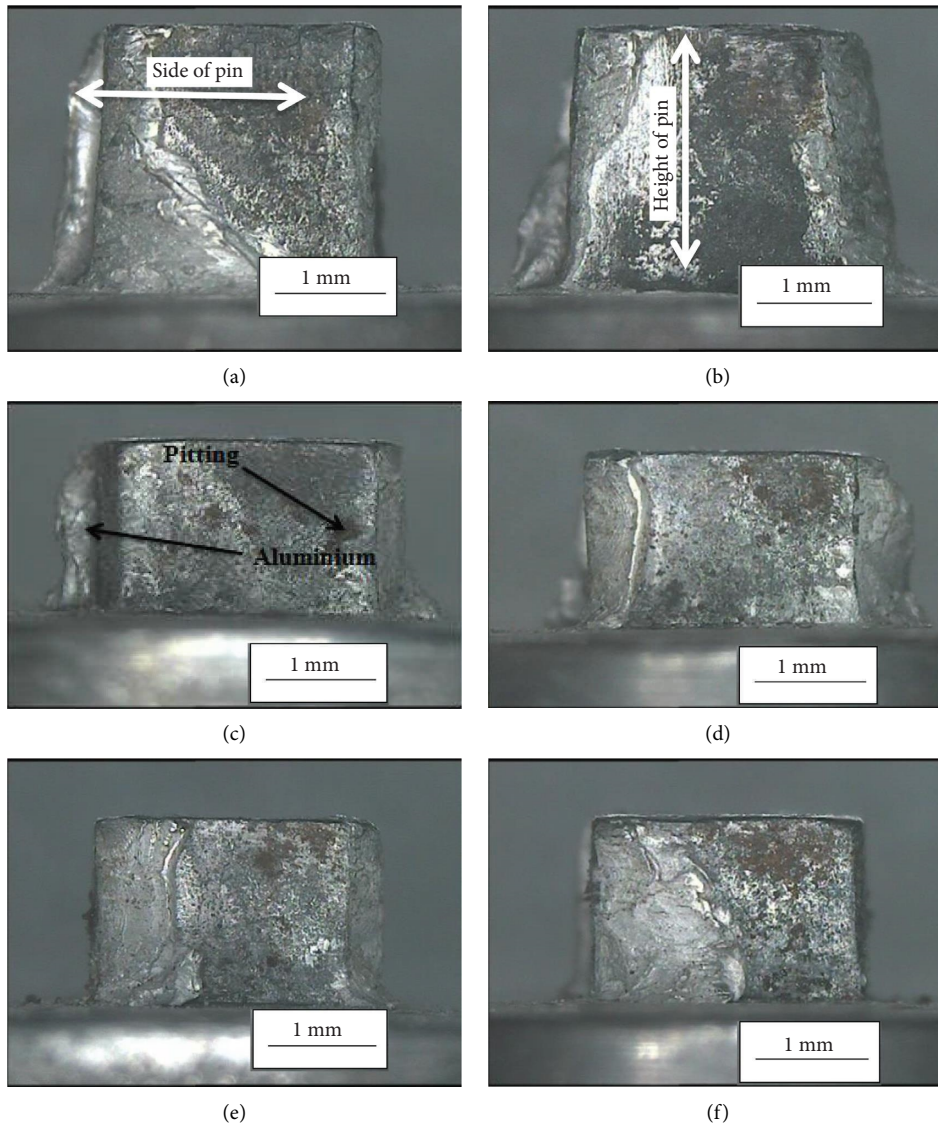
(a)

(b)

(c)

(d)

(e)

(f)

Figure 8: Condition of the tool after welding (a-c) TiN coated Tool, (d-f) DLC coated tool.

Figure 9: Worn surface of the DLC tool.

TABLE 4: Comparison of test results.

| Tool | Flower pollination algorithm (optimized parameters) | | | | Confirmation test | Prediction model |
	Speed(rpm)	Feed (mm/m)	Axial force (kN)	UTS (MPa)	UTS (MPa)	UTS (MPa)
TiN	1540	20	6	136.40	135.62	135.47
AlCrN	1800	20	6	152.08	150.45	151.62
DLC	1360	55	8	132.42	131.77	131.64

points p_1, p_2, ..., p_n. The putative cluster centre of the normalized data points is calculated as the first stage of the procedure. Equation (3) is used to calculate the potential of a p_i data point.

$$p_i = \sum_1^n e^{-\sigma} \|p_i - p_j\|^2,$$

$$\text{Where } \sigma = \frac{4}{r_a^2}. \tag{4}$$

The neighborhood's range is controlled by the value r_a, which is a positive constant. After computing all of the potentials for each data point, the cluster centre with the highest potential is chosen as the initial cluster centre. The second step is to use equation (5) to revise the potential for the available data points other than the designated cluster centre. The cluster centre is determined after the largest potential value point. The neighborhood range is controlled by the constant r_b, which is set at 1.5 times r_a.

$$p_i = p_i - p_i * e^{-\beta} \|p_i - p_j\|^2,$$

$$\text{Where } \beta = \frac{4}{r_b^2}. \tag{5}$$

Finally, the preceding two processes are repeated iteratively until all of the data falls inside the threshold range $(\epsilon) = 0.5$ to any cluster centre. Fuzzy subtractive clustering is implemented in MATLAB using the "genfis" options. The input membership function for each fuzzy cluster is in Gaussian format, and one rule is constructed for each fuzzy cluster based on subtractive clustering. Based on a precise fuzzy modeling method, a fuzzy inference system developed using "genfis" options may predict the output parameter. As a confirmation test, the anticipated values were compared to the optimized values, and experiments were undertaken for the optimized parameters. Table 4 shows the outcomes of the tests compared.

When the predicted values were compared to the experimental values, the root mean square error (RSME) of TiN, AlCrN, and DLC was found to be 0.0027, 0.0016, and 0.0015, respectively, indicating that the UTS prediction based on fuzzy subtractive clustering approach is excellent and effective.

4. Conclusion

Using three coated tools with varying friction coefficients and hardness values, an effort was made to join B4C-reinforced AA 5083 metal matrix composites by friction stir welding. The following observations were drawn from the experimental investigation.

(i) Among the three tools, the AlCrN-coated tool produced the maximum tensile strength of 153 MPa followed by the TiN- and DLC-coated tools at 136 MPa and 130 MPa, respectively.

(ii) Even though process parameters were changed at three various levels, for the same tool, the tensile strength was not changed drastically. On contrary, among the three tools, a noticeable variation was observed and this variation was due to the change in the friction coefficient of the tool coating.

(iii) The flower pollination algorithm (FPA) was used to find the optimized process parameters, and the results were tested by doing a confirmation test on the optimized process parameters. These test results were also compared to the predicted values, and the percentage variation was found to be less than 5%. The results proved that the optimization method and prediction models were accurate.

(iv) The microstructural analysis of weldments prepared by the TiN-coated tool showed small agglomeration of reinforcement particles. The stir zone of the specimen had elongated grains due to plastic deformation. At a larger friction coefficient, higher rotational speed, and lower traverse feed, more amount of heat was developed and aluminium particles got stuck on the tool surface which was reflected as small tunnels and voids. Due to the nominal friction coefficient, the AlCrN-coated tool induced effective stirring. The optical microstructure showed clear distinct regions and observed onion rings near the stir zone.

(v) For the DLC-coated tool, due to the minimum friction coefficient, the amount of heat developed was less, which affected the stirring of the process.

(vi) The condition of the tool was analyzed by the images taken using the video measuring system. The TiN-coated tool undergoes maximum sticking phenomenon in which the aluminium particles got stuck to the surface of the tool pin due to the higher friction coefficient. The results revealed that the AlCrN-coated tool was subjected to partial sliding and partial sticking. The DLC-coated tool underwent full sliding where the extrusion of the material was carried fully by the tool pin which resulted in tool wear.

(vii) The results of the fuzzy clustering showed that the technique was effectively used in predicting the

ultimate tensile strength with the root mean square error (RMSE) values of 0.0027, 0.0016, and 0.0015 for TiN, AlCrN, and DLC coated tools, respectively. The minimum RMSE values indicated that the clustering technique can be effectively used to predict the ultimate tensile strength for any parameters within the range without conducting the experiments to save money and time.

Data Availability

The data used to support the findings of this study are included within the article.

Conflicts of Interest

The authors declare that they have no conflicts of interest.

References

[1] K. Dinesh Kumar, G. Agnihotri, and R. Purohit, "Advanced aluminium matrix composites: the critical need of automotive and aerospace engineering field," *Materials Today Proceedings*, vol. 2, pp. 3023–3041, 2015.

[2] F. Nturanabo, M. Leonard, and J. Baptist Kirabira, "Novel applications of aluminium metal matrix composites," *Aluminum Alloys and Composites*, pp. 1–24, 2019.

[3] S. Gopalakrishnan and N. Murugan, "Prediction of tensile strength of friction stir welded aluminium matrix TiCp particulate reinforced composite," *Materials and Design*, vol. 32, no. 1, pp. 462–467, 2011.

[4] A. Heidarzadeh, S. Mironov, R. Kaibyshev et al., "Friction stir welding/processing of metals and alloys: a comprehensive review on microstructural evolution," *Progress in Materials Science*, vol. 117, Article ID 100752, 2021.

[5] V. P. Singh, S. K. Patel, A. Ranjan, and B. Kuriachen, "Recent research progress in solid state friction-stir welding of aluminium–magnesium alloys: a critical review," *Journal of Materials Research and Technology*, vol. 9, no. 3, pp. 6217–6256, 2020.

[6] D. kumar Rajak, D. D. Pagar, P. L. Menezes, and A. Eyvazian, "Friction-based welding processes: friction welding and friction stir welding," *Journal of Adhesion Science and Technology*, vol. 34, no. 24, pp. 2613–2637, 2020.

[7] V. K. Parikh, A. D. Badgujar, and N. D. Ghetiya, "Joining of metal matrix composites using friction stir welding: a review," *Materials and Manufacturing Processes*, vol. 34, no. 2, pp. 123–146, 2018.

[8] A. M. Hassan, M. Almomani, T. Qasim, and A. Ghaithan, "Effect of processing parameters on friction stir welded aluminum matrix composites wear behavior," *Materials and Manufacturing Processes*, vol. 27, no. 12, pp. 1419–1423, 2012.

[9] S. J. Vijay and N. Murugan, "Influence of tool pin profile on the metallurgical and mechanical properties of friction stir welded Al–10 wt.% TiB2 metal matrix composite," *Materials and Design*, vol. 31, no. 7, pp. 3585–3589, 2010.

[10] G. Nandipati, N. Rao Damera, and R. Nallu, "Effect of Microstructural changes on Mechanical properties of Friction stir welded Nano SiC reinforced AA6061composite," *International Journal of Engineering Science and Technology*, vol. 2, no. 11, pp. 6491–6499, 2010.

[11] Y. Bozkurt, "Weldability of metal matrix composite plates by friction stir welding at low welding parameters," *Materials Technology*, vol. 45, no. 5, pp. 407–412, 2010.

[12] I. Dinaharan and N. Murugan, "Automation of friction stir welding process to join aluminum matrix composites by optimization," *Procedia Engineering*, vol. 38, pp. 105–110, 2012.

[13] F. Cioffi, R. Fernandez, D. Gesto, P. Rey, D. Verdera, and G. Gonzalez Doncel, "Friction stir welding of thick plates of aluminum alloy matrix composite with a high volume fraction of ceramic reinforcement," *Composites Part A: Applied Science and Manufacturing*, vol. 54, pp. 117–123, 2013.

[14] P. Periyasamy, B. Mohan, V. Balasubramanian, S. Rajakumar, and S. Venugopal, "Multi-objective optimization of friction stir welding parameters using desirability approach to join Al/SiCp metal matrix composites," *Transactions of Nonferrous Metals Society of China*, vol. 23, no. 4, pp. 942–955, 2013.

[15] K. S. A. Ali, V. Mohanavel, S. A. Vendan et al., "Mechanical and microstructural characterization of friction StirWelded SiC and B_4C reinforced aluminium alloy AA6061 metal matrix composites," *Materials*, vol. 14, no. 11, p. 3110, 2021.

[16] L. Prasad, A. Kumar, R. Jaiswal, A. Kumar, V. Kumar, and A. Yadav, "Mechanical properties of AA6061T6 and AA6351T6 plates joined by friction stir welding," *Materialwissenschaft und Werkstofftechnik*, vol. 53, no. 8, pp. 888–896, 2022.

[17] A. Yadav, A. Ghosh, and A. kumar, "Experimental and numerical study of thermal field and weld bead characteristics in submerged arc welded plate," *Journal of Materials Processing Technology*, vol. 248, pp. 262–274, 2017.

[18] F. Hasan, R. Jaiswal, A. Kumar, and A. Yadav, "Effect of TiC and graphite reinforcement on hardness and wear behaviour of copper alloy B-RG10 composites fabricated through powder metallurgy," *JMST Advances*, vol. 4, pp. 1–11, 2022.

[19] U. M. Rao, Y. R. Sood, and R. K. Jarial, "Subtractive clustering fuzzy expert system for engineering applications," *Procedia Computer Science*, vol. 48, pp. 77–83, 2015.

[20] K. Ali, F. Sarmadian, A. Rahmani, A. Ahmadi, R. Labbafi, and A. Muhammad Iqbal, "Fuzzy clustering analysis for modeling of soil cation exchange capacity," *Australian Journal of Agricultural Engineering*, vol. 3, no. 1, pp. 27–33, 2012.

[21] A. Yazdani Chamzini, M. Razani, S. H. Yakhchali, E. K. Zavadskas, and Z. Turskis, "Developing a fuzzy model based on subtractive clustering for road header performance prediction," *Automation in Construction*, vol. 35, pp. 111–120, 2013.

[22] K. B. Pathak and D. M. Adhyaru, "Performance analysis of fuzzy subtractive clustering based MRAC," *International Journal of Applied Engineering Research*, vol. 13, no. 9, pp. 6766–6770, 2018.

[23] B. Olawoye, *A Comprehensive Handout on Central Composite Design (CCD), Ife*, Obafemi Awolowo University, Nigeria, 2016.

[24] O. K. Meng, O. Pauline, S. C. Kiong, H. A. Wahab, and N. Jafferi, "Application of modified flower pollination algorithm on mechanical engineering design problem," *IOP Conference Series: Materials Science and Engineering*, vol. 165, Article ID 012032, 2017.

[25] N. Dialami, M. Cervera, and M. Chiumenti, "Defect formation and material flow in Friction stir welding," *European Journal of Mechanics, A Solids*, vol. 80, Article ID 103912, 2020.

[26] S. Muthukumaran and S. K. Mukherjee, "Multi-layered metal flow and formation of onion rings in friction stir welds," *The*

International Journal of Advanced Manufacturing Technology, vol. 38, no. 1-2, pp. 68–73, 2008.

[27] Y. Sun, W. Liu, Y. Li, W. Gong, and C. Ju, "The influence of tool shape on plastic metal flow, microstructure and properties of friction stir welded 2024 aluminum alloy joints," *Metals*, vol. 12, no. 3, p. 408, 2022.

[28] S. Yaknesh, M. Tharwan, R. Saminathan et al., "Mechanical and Microstructural Investigation on AZ91B Mg Alloys with Tool Tilt Variation by Friction Stir Welding," *Advances in Materials Science and Engineering*, vol. 2022, Article ID 831143, 14 pages, 2022.

[29] A. Kumar, A. Yadav, and J Winczek, "Investigation of deformation behaviour of steel, aluminium and copper alloys during hydro – mechanical drawing," *Archive of Mechanical Engineering*, vol. 69, no. 3, 2021.

[30] A. Abebe Emiru, D. K. Sinha, A. Kumar, and A. Yadav, "Fabrication and characterization of hybrid aluminium (Al6061) metal matrix composite reinforced with SiC, B4C and MoS2 via stir casting," *International Journal of Metalcasting*, vol. 17, no. 2, pp. 801–812, 2022.

[31] D. Ibrahim, "An overview of soft computing," *Procedia Computer Science*, vol. 102, pp. 34–38, 2016.

[32] K. Dilip prathihar, *Soft Computing Fundamentals and Application*, Narosa publication, Delhi, India, 2015.